第33卷第6期
2014年12月

红外与毫米波学报
J. Infrared Millim. Waves

Vol. 33, No. 6
December, 2014

文章编号:1001-9014(2014)06-0591-07

DOI:10.3724/SP.J.1010.2014.00591

Formaldehyde and methane spectroscopy measurements based on Mid-IR quantum cascade laser system

WANG Ling-Fang

(Key Laboratory of Optical Fiber Sensing & Communication Ministry of Education, School of Communication and Information Engineering, University of Electronic Science and Technology of China, Chengdu 611731, China)

Abstract: The absorption spectra of H_2CO were recorded at room temperature with a typical equivalent sensitivity of $3.61 \times 10^{-6} cm^{-1} Hz^{-1/2}$ by utilizing a QCL based gas detection set-up. Relative frequency calibration based on F-P etalon and absolute frequency calibration based on CH_4 spectrum are calculated and shown in this paper. Frequency tuning spectra are also measured and processed when changing the operation temperature from -15 ℃ to 20 ℃ with increment of 5 ℃. As nonabsorbent gases, He, Ne, Kr, O_2 and CO_2 were used to determine the line intensity of H_2CO line centered at 1 253.143 92 cm^{-1}. Buffering spectrum in N_2 and the corresponding statistical residuals were given to show broadening characteristics and the difference between the observed absorption data and the expected Voigt fit value with increasing the pressure of buffer gas.

Key words: mid-infrared spectroscopy, distribute feedback-quantum cascade laser, formaldehyde, methane, frequency calibration

PACS: 33.20.Ea

基于中红外量子级联激光器系统的甲醛和甲烷光谱检测

王玲芳

(电子科技大学 通信与信息工程学院光纤传感与通信教育部重点实验室,四川 成都 611731)

摘要:采用相对灵敏度为 3.61×10^{-6} $cm^{-1} Hz^{-1/2}$ 的 QCL 气体检测系统对室温下的甲醛气体进行了吸收光谱的测试,采用 F-P 标准具对系统进行相对频率校准,根据此波段甲烷的吸收谱线对甲醛吸收光谱进行绝对频率校准.当调谐 QCL 工作温度为 -15 ℃ ~20 ℃,以每 5 ℃变化时,采集并处理相应的频率调谐光谱.采用 He, Ne, Kr, O_2 和 CO_2 作为本波段的非吸收性缓冲气体作用于甲醛,通过计算光谱数据得出 1 253.143 92 cm^{-1} 处甲醛的吸收线强度.给出了 N_2 中的展宽光谱以及相应的光谱数据处理残差结果,并对结果进行了分析.

关 键 词:中红外光谱;分布反馈式量子级联激光器;甲醛;甲烷;频率校准

中图分类号:O657.33 **文献标识码**:A

Introduction

Trace-gas analysis and chemical sensing using quantum cascade lasers (QCLs) has attracted great attention in recent years since most molecules have a unique absorption spectrum in the mid-infrared (mid-IR) region[1-2]. With many commercial options available, QCLs are ideal candidates for mid-IR spectroscopy, because their emission wavelength ranges from the mid-IR to the far-IR with high power efficiency since the invention of the QCL decades ago[3], an impressive progress has been achieved from first low temperature pulsed emission to continuous wave operation at room temperature. Formaldehyde (H_2CO) is a carcinogenic pollutant emitted as an intermediate product in the oxidation of most biogenic and anthropogenic hydrocarbons. It is also known as a primary emission product of incomplete hydrocarbon combustion[4-11]. Thus, spectroscopy measurements on H_2CO play important roles both in industrial fields and human safety and health[12-14].

There is no available H_2CO data in the HITRAN

Received date: 2013-11-21, **revised date**: 2014-10-08 **收稿日期**:2013-11-21, **修回日期**:2014-10-08

Foundation items: Supported by National Natural Science Foundation of China(61205067, 61307088), and the Fundamental Research Funds for the Central Universities(ZYGX2013J007, ZYGX2012J008)

Biography: WANG Ling-Fang(1984-), female, Sichuan Chengdu of China, Ph. D. Research involves in infrared integrated optical, infrared spectrometer and other related fields. E-mail: lf.wang@uestc.edu.cn

spectroscopic database[15-16] at wavelength around 8 μm. Therefore in order to get a reference line position, F-P etalon based relative frequency calibration and absorptions of both CH_4 and H_2CO based absolute frequency calibration were utilized and measured. Temperature tuning spectrum, pressure broadening characteristics were given to show more detailed spectroscopy of H_2CO, also intensity of line centered at 1 253.143 92 cm^{-1} was measured and determined based on a distribute feedback quantum cascade laser (DFB-QCL) in this paper.

1 Pulsed DFB-QCL based experimental

Spectra shown in this paper were detected by a pulsed 8 μm DFB-QCL based experimental set-up. The QCL was chosen to emit in a single spectral (linearly polarized, I_0) mode at around 8 μm which can be operated from -40 ℃ to + 40 ℃, then the corresponding wavelength range obtained was 1 248 cm^{-1} to 1 257 cm^{-1}. The laser was operated at 2% duty cycle in pulsed mode with 190 ns pulse duration.

For the experimental set-up (shown in Fig. 1), the laser light was collimated using an off-axis parabolic gold mirror and then passed through a 90 cm long single-pass glass cell filled with the sample gas for detection. The single-pass cell is fitted with BaF_2 windows. Transmitted light from the DFB-QCL was focused by an off-axis parabolic silver mirror (156 mm focal length), then to the optical collimating system and gas cell, then onto a thermoelectrically cooled MCT detector (VIGO PCI-3TE-10/12) with fast preamplifier (Neoplas Control). This was connected to a 2 Gs/s, 350 MHz bandwidth digitizing oscilloscope (LeCroy Wavesurfer 434) which recorded the spectra obtained. All the experiments described in this paper were carried out at the temperature of 296 K.

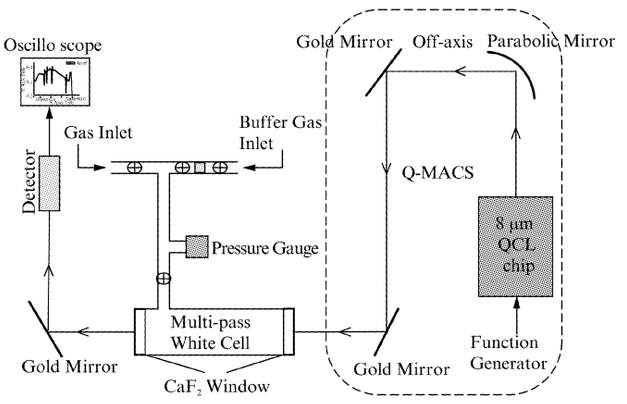

Fig. 1 Schematic diagram of experimental set-up for spectroscopy measurement

图1 红外光谱测试实验系统框图

2 Spectroscopy of formaldehyde measurements

2.1 Relative frequency calibration based on F-P etalon

Before each experiment the frequency chirp was characterized in order to allow the application of a frequency scale to the measured spectra. The radiation was passed through a germanium Fabry-Pérot etalon with a free spectral range of 500 MHz. The longitudinal modes supported by an etalon of length d and refractive index n are separated by the free spectral range shown in Eq. (1)

$$\mathrm{FSR} = \frac{c}{2 \cdot n \cdot d} \quad . \quad (1)$$

A typical signal detected when a 190 ns long laser pulse at a wavelength around 8 μm is passed through an etalon is shown in Fig. 2 (a). Since the pulse signal and the laser is not always coupled ideally at the front of the etalon signal, then range from the middle (see Fig. 2 (b)) would be better to use. Plotted on the same figure is the signal detected from an identical pulse when an empty cell was placed in the beam path.

The frequency scale is obtained by counting the etalon fringes and plotting the corresponding frequency as a function of time, as shown in Fig. 3 plotted by scatters. Fitting polynomial to the plotted scatters, corresponding relative frequency was obtained as

$$y = \mathrm{Intercept} + B_1 \cdot x^1 + B_2 \cdot x^2 + B_3 \cdot x^3 \quad , (2)$$

where y is the relative frequency in GHz, x is time in s. The parameters and values are listed in Table 1. By knowing the relative frequency function, the corresponding wavenumber can be calculated.

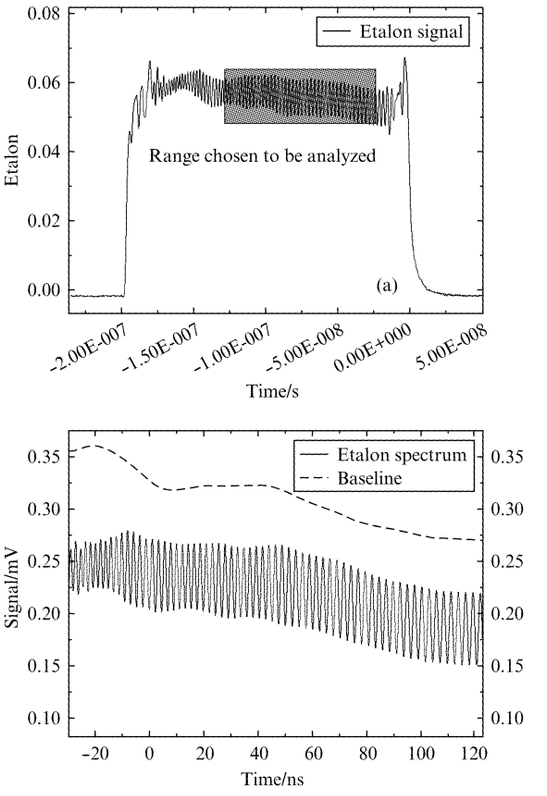

Fig. 2 (a) Signal selected for polynomial function fit, and (b) signal selected from (a) for polynomial function fit is compared with baseline

图2 (a) 选取标准具信号中用于多项式拟合的部分, (b) 并与背景基线作对比

2 Torr methane with purity of 99.9% was introduced into the 90 cm gas cell, and four obvious absorption lines were acquired in the detection range. The application of this conversion in Eq. (2) along with the Beer-Lambert relation allows the measured transmitted intensity and measured or fit incident intensity to be converted into a spectral absorbance trace, see example in Fig. 3(a) of CH_4 absorbance as a function of time, and absorbance as a function of relative frequency in Fig. 4 (b). However, the spectra shown in Fig. 4 (b) even in the frequency domain, lines marked by "a", "b", "c" and "d" still cannot be used in the spectrum analysis and calculation, as the line positions are not those who accurately located, so absolute frequency still need to be done. These additional "wiggles" are an indication that rapid passage processes are taking place. The rapid passages effect was fist observed using an intrapulse spectrometer by Duxbury *et al.*[17], which was an emission spike followed by a series of oscillations to the side of the normal absorption profile as coherent radiation is swept through a transition. However, these rapid passage effects are removed upon addition of a non-absorbing buffer gas.

Table 1 Parameters from polynomial fit results
表 1 多项式拟合结果所得参数

Parameter	Value	Standard Error
Intercept	−10.793 97	0.067 55
B_1	$2.362\,58\times10^{8}$	$1.328\,53\times10^{6}$
B_2	$-2.048\,76\times10^{14}$	$6.001\,03\times10^{12}$
B_3	$-6.746\,3\times10^{7}$	$1.976\,06\times10^{6}$

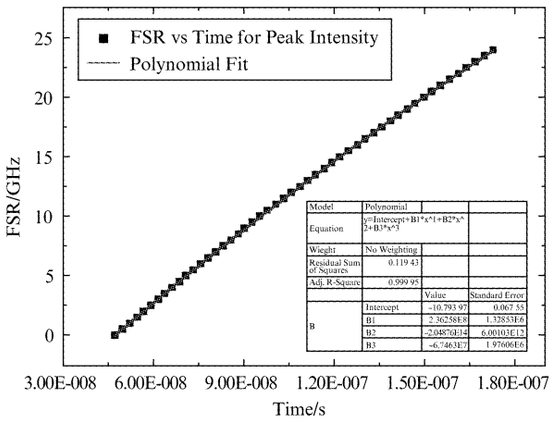

Fig. 3 FSR as a function of time and the polynomial function fit for the etalon signal
图 3 FSR 与时间的函数以及对标准具信号的多项式拟合结果

2.2 Absolute frequency calibration based on CH_4 spectrum

Methane absorption spectrum was simulated based on HITRAN 2008 database[18] with parameters shown in Table 2 and compared with the spectral lines in Fig. 4 (b). The etalon signal was used for relative frequency determination.

The absolute frequency was fixed by the known line-centre frequencies for the v4 band P(8) located in 1 253.349 1 cm^{-1}. Therefore the spectrum is put to an absolute scale through measuring the known CH_4 spectrum and assigning the peaks using the HITRAN database.

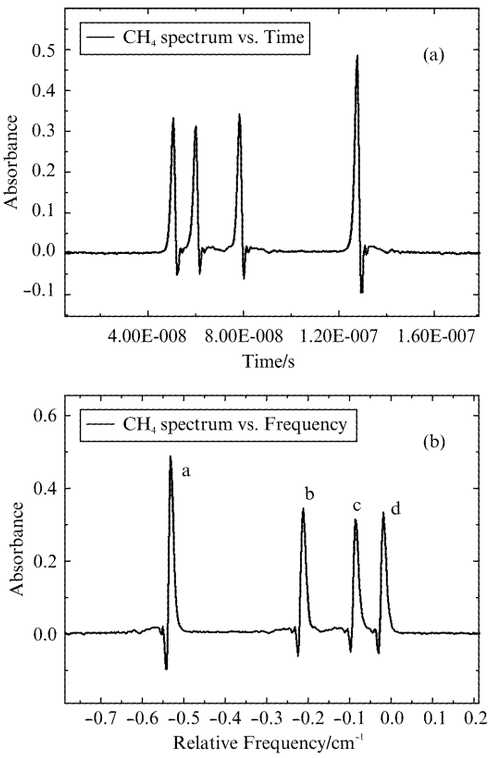

Fig. 4 Absorption spectrum of methane as a function of Time (a), and Relative Frequency (b)
图 4 甲烷气体的(a)吸光度与时间的函数以及(b)与相对频率的函数

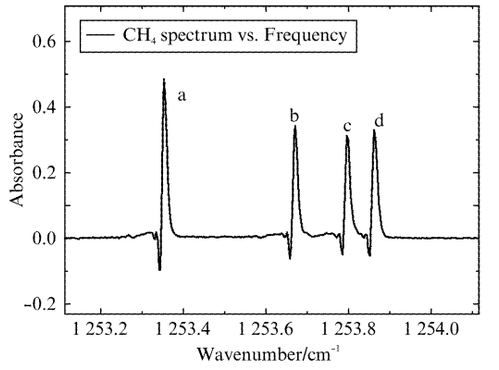

Fig. 5 Absorption spectrum of methane after absolute frequency scale calibration
图 5 进行频率校正后的甲烷吸收光谱

Table 2 Corresponding parameters and values from HITRAN simulation
表 2 基于 HITRAN 数据库仿真所得的相关参数及数值

Parameters	Line a	Line b	Line c	Line d
Transition	v4 P(8)	v4 P(9)	v4 P(8)	v4 P(9)
Line center position(cm^{-1})	1 253.349 1	1 253.661 5	1 253.789 1	1 253.851 1
Line Intensity(cm^{-1}/cm^{-2}molecule)	2.08×10^{-20}	1.55×10^{-20}	1.39×10^{-20}	1.55×10^{-20}

The four absorption lines in Fig. 5 are in the same order as in Fig. 4(b), but the only difference is that their line positions have been calibrated into their accurate center frequency in the absolute frequency scale. Till now the spectral data can be used to determine line parameters such as pressure broadening coefficients and pressure induced line center shift coefficients.

2.3 Laser frequency tuning characteristics based on formaldehyde spectroscopy

Tuning the frequency of the laser across the absorption line is desirable for most of the spectroscopic measurements. Characterization of tuning properties and measuring the tuning rates is therefore important. In QC lasers there are no effects such as carrier density dependent index of refraction, therefore no direct current tuning is observed. The only tuning mechanism is temperature tuning of the index of refraction of the waveguide that changes the apparent optical length of the wavelength selection grating.

As there is no H_2CO absorption spectral data at the wavelength around 8 μm in HITRAN database, we need to calibrate the absolute frequency scale by using other well known gas. In the previous research work[19], we have presented PGOPHER simulation in this detection region as well as using experimental method to calibrate the H2CO frequency scale.

Both CH_4 and H_2CO were introduced into the gas cell, mixed spectra plotted with "— · —" were obtained as shown in Fig. 6, and the 98% purity of formaldehyde along with 99 % purity of methane were also measured separately, their spectra with "——" and "- - -" were plotted in the same figure. The absolute frequency was fixed by the known line-centre frequencies for the $v4$ band P(8), P(9) and P(8) lines located in 1 253.349 1 cm^{-1}, 1 253.661 5 cm^{-1} and 1 253.789 1 cm^{-1} respectively.

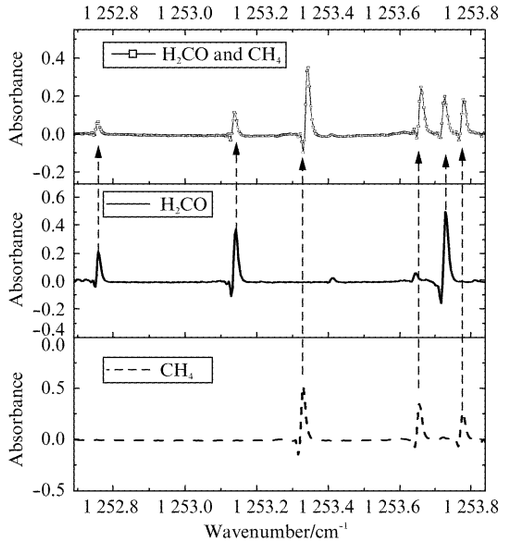

Fig. 6 Both H_2CO and CH_4 spectrum were measured in the same gas cell, and their line positions were compared
图6 同一气室中测得的甲醛和甲烷气体的吸收光谱

Line positions of H_2CO absorption lines can be determined even one line center frequency was calibrated. Tuning the operation temperature of DFB-QCL from −15 ℃ to +20 ℃ with increment of 5 ℃, the sweeping spectra in each spectral range were obtained as shown in Fig. 7, plotted on the top of the figure is the qualitative data from PNNL[20] by using FTIR spectrometer. It is obvious from Fig. 7 that the spectra obtained from the QCL system has a higher resolution than that obtained from FTIR scanned qualitative data in PNNL. The resolution can be found out by substituting the results from Voigt and linear fits to the spectrum of formaldehyde into the sensitivity equation. The relative wide spectral range of 1 250 ~ 1 254.5 cm^{-1} was obtained and numbers of absorption lines were detected for intensive measurement or as a reference for the person who work in this research area and are interest in the H_2CO detection.

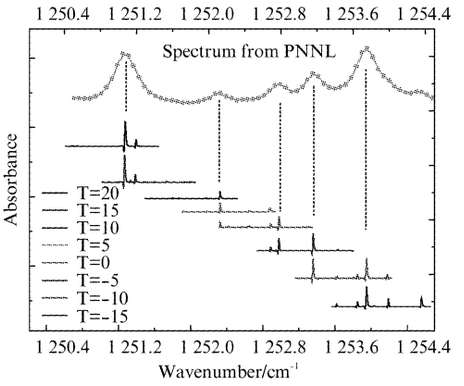

Fig. 7 Temperature sweeping spectrum at operation temperatures from −15 ℃ to +20 ℃ with increment of 5 ℃
图7 从−15 ℃至20 ℃ 以每隔5 ℃改变时甲醛的扫描光谱

Depictured in Fig. 8 is the 3D view of temperature sweeping spectra from which we can have a direct impression about H_2CO absorbance as functions of both wavenumber and temperature.

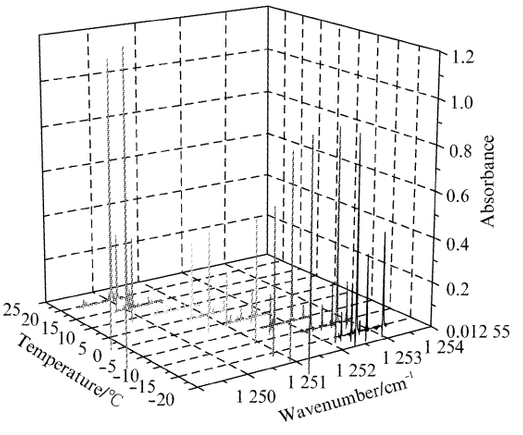

Fig. 8 3D-view absorption spectra of formaldehyde in temperature sweeping
图8 甲醛温度扫描光谱的3D视图

For temperature sweeping spectrum, calculation of the tunable line center position as a function of operate temperature had been done and the temperature tunable

coefficient was obtained as $-0.083\ 09\ cm^{-1}/K$. Results can be seen in Fig. 9.

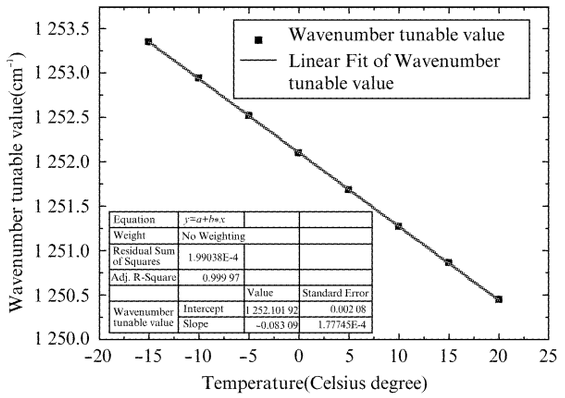

Fig. 9　Tunable central emission frequency as a function of sweeping temperature

图 9　可调谐中心频率与扫描温度的函数及线性拟合结果

2.4　Line intensity measurements

The strength of a line can often be determined by a direct method from the line center absorption. The Beer-Lambert absorbance is expressed as Eq. 3,

$$A = -\ln\left(\frac{I}{I_o}\right) = -\ln\left(e^{-\alpha(\upsilon)L}\right) = \alpha(\upsilon)L = \sigma(\upsilon)CL \quad , \quad (3)$$

where I and I_o are the intensities of transition with and without absorption of gas of interest, $\alpha(\upsilon)$ is the absorption coefficient, L is the optical path length, C is the concentration, and $\sigma(\upsilon)$ is the absorption cross section. The integral of the spectrum over a given frequency range allows the integrated cross section to be obtained using $\sigma_{int} = \int A(\upsilon)\,d\upsilon/CL$ and then $\int A(\upsilon)\,d\upsilon$ will be given in the form of "integrated area" which should not change theoretically because of the fixed H_2CO amount when the spectral line is broadened by introducing buffer gas into the cell. Using the Eq. 3 deduced above the integrated cross sections were evaluated at each buffer gas pressure both in single cell experimental system and White cell system, plotted in Fig. 10, results observed with buffering by He, Ne, Kr, O_2 and CO_2 are shown in Table 3.

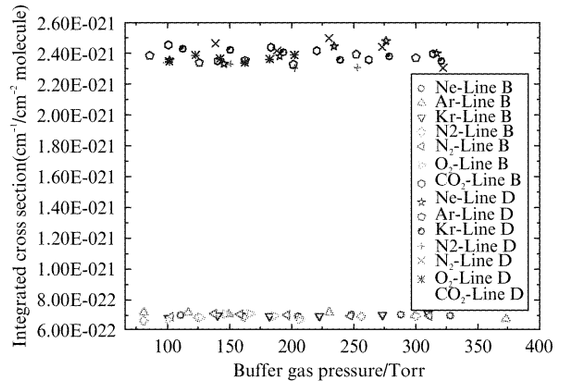

Fig. 10　Plots of integrated cross section as a function of buffer gas pressure for He, Ne, Ar, Kr, N_2, O_2 and CO_2

图 10　吸收线强度与缓冲气体压强的函数关系

Table 3　Integrated cross sections of H_2CO in He, Ne, Kr, O_2 and CO_2 buffering experiments, which were measured in 90 cm single cell at 296 K

表 3　在 90 cm 气室中所测得的 H_2CO 与 He, Ne, Kr, O_2和 CO_2 相互作用下的吸收线强度

Line Intensity (cm^{-1}/cm^{-2}molecule)	Line B (1,1,1←2,0,2)	Line D (10,1,9←9,2,8)
σ_{H_2CO-He}	$(6.97\pm0.13)\times10^{-22}$	$(2.41\pm0.12)\times10^{-21}$
σ_{H_2CO-Ne}	$(6.98\pm0.18)\times10^{-22}$	$(2.37\pm0.14)\times10^{-21}$
σ_{H_2CO-Ar}	$(6.96\pm0.13)\times10^{-22}$	$(2.38\pm0.13)\times10^{-21}$
σ_{H_2CO-Kr}	$(6.99\pm0.14)\times10^{-22}$	$(2.39\pm0.11)\times10^{-21}$
$\sigma_{H_2CO-N_2}$	$(6.98\pm0.13)\times10^{-22}$	$(2.40\pm0.13)\times10^{-21}$
$\sigma_{H_2CO-O_2}$	$(7.02\pm0.16)\times10^{-22}$	$(2.41\pm0.15)\times10^{-21}$
$\sigma_{H_2CO-CO_2}$	$(6.91\pm0.17)\times10^{-22}$	$(2.35\pm0.12)\times10^{-21}$
σ_{avg}	$(6.97\pm0.16)\times10^{-22}$	$(2.39\pm0.13)\times10^{-21}$

2.5　Characteristics of nitrogen buffering spectrum

Pressure broadening parameters of H_2CO in 7 non-absorbent gases have been discussed in the previous work, and now we just show the buffering spectrum characteristics in two situations which are fixed amount of H_2CO with different pressures of N_2 and fixed amount of N_2 with different pressures of H_2CO.

2.5.1　Different pressures of N_2 with fixed amount of H_2CO

3 Torr 98% formaldehyde and N_2 were both introduced into the gas cell, then keep the amount of H_2CO fixed with increasing amount of N_2 from 90 Torr to 174 Torr, 253 Torr and 396 Torr. Spectrum from each situation was acquired separately and series of spectra were depictured in Fig. 11. When the pressure of N_2 increased, the H_2CO absorption spectrum is broadened and rapid passage effect also become more unobvious.

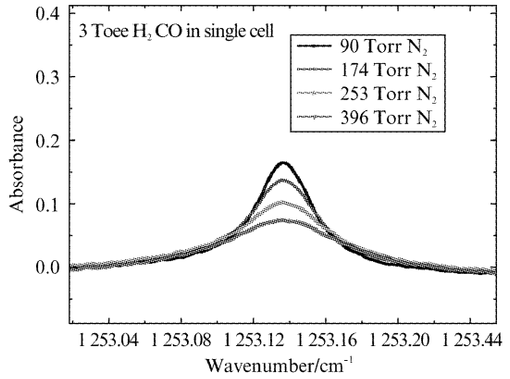

Fig. 11　Fixed amount of H_2CO with different pressures of N_2

图 11　相同量的甲醛与不同量的氮气相互作用下的光谱

Statistical residual describes the difference between the observed absorption data and the expected Voigt fit value and may be plotted as a function of frequency which is shown in Fig. 12. As is evident from the figure, the residual reduces with increasing buffer gas pressure as the rapid passage decreases, so it shows the better

Voigt fit results will be the higher pressure of buffer gas will be used and the pressure broadening coefficients will be more accurate.

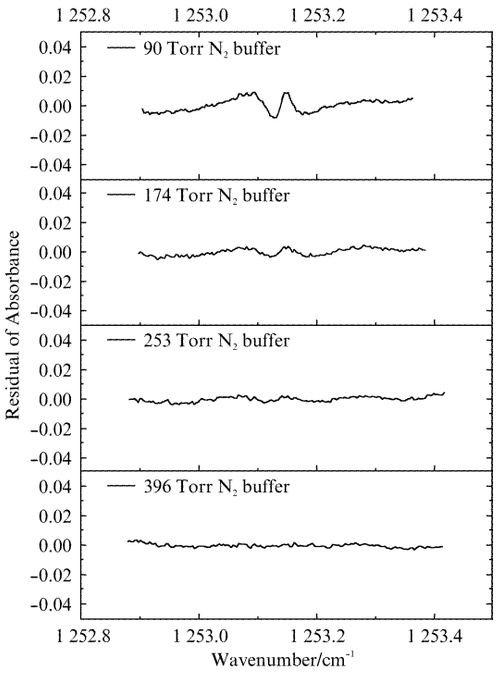

Fig. 12 Residuals of Voigt fit to H_2CO lineshape where 3 Torr H_2CO was buffered with 90, 174, 253 and 396 Torr of N_2 in the 90 cm single cell

图 12 3 Torr 甲醛分别与 90、174、253 和 396 Torr N_2 相互作用的吸收光谱的 Voigt 拟合残差

2.5.2 Fixed amount of N_2 with different pressures of H_2CO

Pressure broadening effects are normally measured by fixing the amount of gas of interest and then introducing different pressures of buffer gas. In this work, fixing of buffer gas amount and changing the amount of H_2CO was used to check the broadening effect. Different pressures (2.6, 4 and 5 Torr) of H_2CO were separately introduced into the gas cell with a fixed amount of N_2 (100 Torr).

Spectra were acquired and fit to a Voigt function, and then the residuals of the absorbance are determined, which can be seen in Fig. 13. The residuals increased as the H_2CO pressure increases. In both sets of experiments, the residual decreases when the ratio of buffer gas pressure to H_2CO pressure increases as the significance of the rapid passage effects declines.

3 Conclusions

The work represents the relative frequency calibration based on F-P etalon along with HITRAN database simulation and absolute frequency calibration based on CH_4 spectrum. Temperature tuning characteristics were shown by 2D and 3D figures, and tuning parameter was determined as $-0.083\ 09\ cm^{-1}/K$ when sweeping the

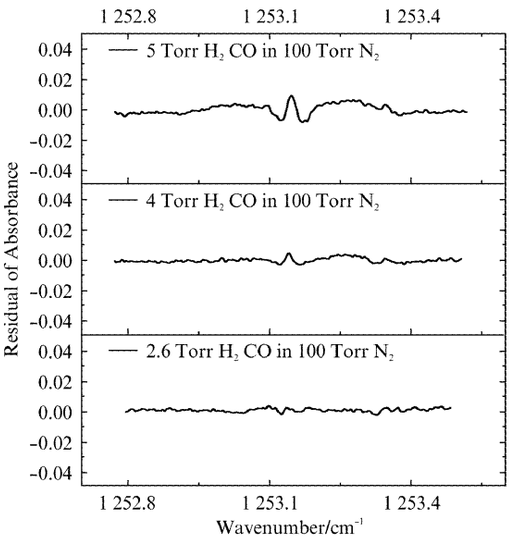

Fig. 13 Residuals of different pressures of H_2CO with a fixed amount of N_2: 2.6, 4 and 5 Torr H_2CO buffered with 100 Torr N_2 respectively

图 13 不同量的甲醛与固定量的 N_2 相互作用的吸收光谱的 Voigt 拟合残差

temperature from -15 ℃ to $+20$ ℃, then the corresponding spectral range of 1 250 ~ 1 254.5 cm^{-1} was obtained. Nitrogen buffering spectra with two different situations of fixed amount of H_2CO with different pressures of N_2 and fixed amount of N_2 with different pressures of H_2CO were shown and their Voigt fit statistics residuals were discussed.

References

[1] Steck1 T, Glatthor N, von Clarmann T, *et al*. Retrieval of global upper tropospheric and stratospheric formaldehyde (H_2CO) distributions from high-resolution MIPAS-envisat spectra[J]. *Atmos Chem Phys*. 2008, **8**(3): 463 - 470.

[2] Jacquemart P A, Tchana D K, Lacome F. Laboratory intercomparison of the formaldehyde absorption cross sections in the infrared (1660 - 1820 cm^{-1}) and ultraviolet (300 - 360 nm) spectral regions [J]. *JQSRT*, 2007, **112**(D5): 1 - 10.

[3] Faist J, Capasso F, Sivco D L, *et al*. A trace methane gas sensor using mid-infrared quantum cascaded laser at 7.5 μm[J]. *Science*, 1994, **264**(158): 553 - 556.

[4] Amato P, Demeer F, Melaouhi A, *et al*. A fate for organic acids, formaldehyde and methanol in cloud water: their biotransformation by micro-organisms[J]. *Atmospheric Chemistry and Physics Discussions*. 2007, **7**(2): 5253 - 5276.

[5] Wisthaler A, Apel E C, Bossmeyer J, *et al*. Technical Note: Intercomparison of formaldehyde measurements at the atmosphere simulation chamber SAPHIR[J]. *Atmos. Chem. Phys*. 2008, **8**: 2189 - 2200.

[6] Chane K, Orphal J. Revised ultraviolet absorption cross section of H_2CO for the HITRAN database[J]. *Journal of Quantitative Spectroscopy and Radiative Transfer*. 2011, **112**, 1509 - 1510.

[7] Burling I R, Yolelson R J, Akagi S K, *et al*. Airborne and ground-based measurements of the trace gases and particles emitted by prescribed fires in the United States[J]. *J. Geophys. Res*. 2011, **11**: 12197 - 12216.

[8] Heald C L, Goldstein A H, Allan J D, *et al*. Tropospheric Emissions: Monitoring of Pollution (TEMPO) sites/presentations[J]. *J. Geo-*

phys. Res. Lett. 2008, **8**(7): 2007 - 2025.

[9] Chen X, Cheng L W, Guo D K, *et al.* Quantum cascade laser based standoff photoacoustic chemical detection[J]. *Sensors.* 2011, **9**(21): 20251 - 20257.

[10] Kosterev A, Wysocki G, Bakhirkin Y A, *et al.* Application of quantum cascade lasers to trace gas analysis[J]. *Applied Physics B.* 2008, **90**(2): 165 - 176.

[11] Lin Y C, Schwab J J, Demerjian K L, *et al.* Summertime formaldehyde observations in New York city: Ambient levels, Sources and Its Contribution to HOx Radicals [J]. *J. Geophys. Res.*, 2012, **117** (D8): 1 - 14.

[12] http://www.osha.gov/SLTC/formaldehyde/ [Z], accessed January 2009.

[13] WHO Regional Office for Europe[Z], Copenhagen, Denmark, 2001.

[14] Flueckiger J, Ko F K, Cheung K C. Microfabricated formaldehyde gas sensors[J]. *Sensors.* 2009, **9**(11): 9196 - 9215.

[15] Perrin A, Keller K, Flaud JM. New analysis of the $\nu 2$, $\nu 3$, $\nu 4$ and $\nu 6$ bands of formaldehyde H212C16O line positions and intensities in the 5 - 10 μm spectral region[J]. *J Mol Spectrosc*, 2003, **221**(2): 192 - 198.

[16] Rothman L S, Gordon I E, Barbe A, *et al.* The HITRAN 2004 molecular spectroscopic database[J]. *Journal of Quantitative Spectroscopy & Radiative Transfer.* 2005, **96**: 139 - 204.

[17] Duxbury G, Langford N, McCulloch M T, *et al.* Quantum cascade semiconductor infrared and far-infrared lasers: from trace gas sensing to non-linear optics[J]. *Chem. Soc. Rev.*, 2005, **34**(11): 921 - 934.

[18] Rothman L S, Gordon I E, Barbe A, *et al.* The HITRAN 2008 molecular spectroscopic database[J]. *Journal of Quantitative Spectroscopy & Radiative Transfer.*, 2009, **110**: 533 - 572.

[19] Wang L, Sharples T R. Intrapulse quantum cascade laser spectroscopy: pressure induced line broadening and shifting in the $\nu 6$ band of formaldehyde[J]. *APPL PHYS B.* 2012, **108**(2): 427 - 435.

[20] Pacific Northwest National Laboratory (PNNL)[Z]: https://secure2.pnl.gov/nsd/NSD.nsf/Welcome.OpenForm.